J Physiol 597.21 (2019) pp 5295–5306

The Journal of Physiology

Sniffing behaviour-related changes in cardiac and cortical activity in rats

Nahoko Kuga[1], Ryota Nakayama[1], Yu Shikano[1], Yuya Nishimura[1], Toya Okonogi[1], Yuji Ikegaya[1,2] and Takuya Sasaki[1,3]

[1]*Laboratory of Chemical Pharmacology, Graduate School of Pharmaceutical Sciences, The University of Tokyo, 7-3-1 Hongo, Bunkyo-ku, Tokyo, 113-0033, Japan*
[2]*Center for Information and Neural Networks, Suita City, Osaka, 565-0871, Japan*
[3]*Precursory Research for Embryonic Science and Technology, Japan Science and Technology Agency, 4-1-8 Honcho, Kawaguchi, Saitama, 332-0012, Japan*

Edited by: Kim Barrett & Dario Farina

Key points

- High-frequency (HF) sniffing represents active odour sampling and an increase in the animal's motivation.
- We examined how HF sniffing affects the physiological activity of the brain–body system.
- During HF sniffing, heart rates and the ratio of theta to delta critical local field potential power were comparable to those observed during motion periods.
- Vagus nerve spike rates did not vary depending on HF sniffing.
- Our results suggest that physiological factors in the central nervous system and the periphery are not simply determined by locomotion but are crucially associated with HF sniffing.

Abstract Sniffing is a fundamental behaviour for odour sampling, and high-frequency (HF) sniffing, generally at a sniff frequency of more than 6 Hz, is considered to represent an animal's increased motivation to explore external environments. Here, we examined how HF sniffing is associated with changes in physiological signals from the central and peripheral organs in rats. During HF sniffing while the rats were stationary, heart rates, the magnitude of dorsal neck muscle contraction, and the ratio of theta to delta local field potential power in the motor cortex were comparable to those observed during motion periods and were significantly higher than those observed during resting respiration periods. No pronounced changes in vagus nerve spike rates were detected in relation to HF sniffing. These results demonstrate that central and peripheral physiological factors are crucially associated with the emergence of HF sniffing, especially during quiescent periods. Behavioural data might be improved to more accurately evaluate an animal's internal psychological state if they are combined with a sniffing pattern as a physiological marker.

Nahoko Kuga received her PhD in Pharmaceutical Sciences from The University of Tokyo, Japan in 2018. Currently she is working as a research manager at ERATO IKEGAYA BRAIN-AI Hybrid Project in the Graduate School of Pharmaceutical Sciences at The University of Tokyo.

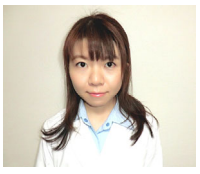

DOI: 10.1113/JP278500

(Received 21 July 2019; accepted after revision 9 September 2019; first published online 12 September 2019)
Corresponding author T. Sasaki: Laboratory of Chemical Pharmacology, Graduate School of Pharmaceutical Sciences, The University of Tokyo, 7-3-1 Hongo, Bunkyo-ku, Tokyo, 113-0033, Japan. Email: tsasaki@mol.f.u-tokyo.ac.jp

Introduction

For rodents, sniffing is a fundamental behaviour that controls active odour sampling (Youngentob *et al.* 1987; Verhagen *et al.* 2007; Wachowiak, 2011). The basic sniffing frequency of a rodent is 1–3 Hz in a resting state, but it can transiently reach up to 12 Hz depending on behavioural demands (Uchida & Mainen, 2003; Kepecs *et al.* 2007; Verhagen *et al.* 2007; Tsanov *et al.* 2014). In behavioural studies, such rapid bouts of nasal inhalation are considered to represent an animal's motivation for exploration and social interactions (Wesson, 2013). While the functional role of sniffing in active sensory sampling has been extensively studied, it remains to be fully clarified how sniffing behaviour affects the physiological activity of the brain–body system.

The aim of this study is to understand how systemic physiological signals in rats undergo changes in conjunction with sniff frequency, especially upon the transient emergence of high-frequency (HF) sniffing. A large number of studies have utilized neck muscle contraction and the power of brain electrical activity as objective measures to estimate an animal's arousal state (Vyazovskiy *et al.* 2009; Hayashi *et al.* 2015; Oishi *et al.* 2016; Watson *et al.* 2016). Heartbeats and autonomic nervous signals are peripheral signals that are finely tuned in response to cognitive demands and psychological states. In particular, since the vagus nerve (VN) is a major autonomic pathway for the transfer of signals between the brain and the peripheral organs, there is a possibility that changes in sniffing patterns might induce changes in ongoing spike patterns of the VN. Unveiling the association of these physiological factors with sniffing behaviour will be helpful for accurately understanding the conventionally hidden physiological activity of the internal organs during observable behavioural patterns.

To this end, we performed simultaneous recordings of local field potential (LFP) signals from the motor cortex and the olfactory bulb (OB), an electrocardiogram (ECG) signal, a dorsal neck muscle electromyogram (EMG) signal, and a VN electrophysiological signal from freely moving rats using our recording technique (Okada *et al.* 2016; Sasaki *et al.* 2017; Shikano *et al.* 2018, 2019). Conventionally, the sniff frequency of rodents is quantified based on respiration-locked intranasal pressure or the temperature of nasal air flow (Clarke *et al.* 1970; Cheung *et al.* 2009). In addition to these measures, LFP signals from the OB have been shown to reflect nasal respiratory cycles nearly perfectly, especially in awake animals (Brankack & Klingberg, 1982; Carlson *et al.* 2014; Rojas-Libano *et al.* 2014; Jessberger *et al.* 2016). By utilizing the features of the OB electrical signal, we defined sniffing events and quantitatively analysed their relation to the dynamics of the other electrophysiological signals.

Methods

Ethical approval

All experiments were performed with the approval of the animal experimental ethics committee at the University of Tokyo (approval number: P29-7) and in accordance with the NIH guidelines for the care and use of animals. All investigators followed the ethical principles outlined in Grundy (2015).

Animals

A total of 10 male Sprague–Dawley rats and 3 male Long Evans rats were purchased from SLC (Shizuoka, Japan). Out of the 10 Sprague–Dawley rats, 5 rats were tested in a familiar home cage and an open field and the other 5 rats were tested in an elevated plus maze test. The Long Evans rats were used for social defeat experiments. The animals were 8–9 weeks old, weighed 296–400 g, had free access to water and food at all times and were maintained under inverted 12 h light/12 h dark conditions (light from 20.00 to 08.00 h). No animals were excluded from our analyses. After the recordings were completed, rats were killed with an overdose of pentobarbital (300 mg kg^{-1}, I.P.).

Electrode preparation and surgery

An electrode assembly including recording and stimulating electrodes was prepared as described previously (Okada *et al.* 2016; Sasaki *et al.* 2017; Shikano *et al.* 2018, 2019). The electrode assembly was composed of an electrical interface board (EIB) (EIB-36-PTB, Neuralynx, Inc., Bozeman, MT, USA) that consisted of an outer cover and a core body, which were custom-made with 3-D printers (UP Plus2, Tiertime, Beijing, China; formlabs Form2, Formlabs, Somerville, MA, USA). The EIB had metal holes (channels), including four LFP channels, two ECG channels, two EMG channels, two VN channels, and two earth (ground)/reference channels, for connecting electrodes. The individual channels were connected to insulated wires (∼5 cm), and the opposite ends of these wires were soldered to individual electrodes during the final step of the surgery.

Anaesthesia was induced with 3% isoflurane gas and then maintained with 1–2% isoflurane gas while the

animals lay on their backs. Buprenorphine (0.05 mg kg^{-1}, S.C.) was given as an analgesic. Veterinary ointment was applied to the rats' eyes to prevent dryness. For all steps of an incision, the skin at the incision site was sterilized with betadine and 70% ethanol. For each rat, an incision was made on the left side of the neck from the larynx to the sternum, and the left cervical VN was enclosed in a custom-made cuff-shaped VN electrode (Unique Medical Co. Ltd, Japan; inner diameter, 0.5–1.0 mm; electrode area, 0.25 mm^2; cathode–anode interval, 1.5–2.0 mm; and total length, 4.0 mm; for more details, see Shikano *et al.* 2019). All rats then underwent surgery to implant the ECG, EMG and LFP electrodes. Briefly, two ECG electrodes (stainless-steel wires; AS633, Cooner Wire Company, CA, USA) were attached to the intercostal muscles on both sides of the chest, and two EMG electrodes were sutured at an interval of ∼1 mm to the dorsal neck area. For EMG and ECG recordings, two electrodes were implanted for a recording in case of an accidental interruption of either one of the electrodes. In these recordings, signals were chosen from a normally working channel. A mid-line incision was made over the skull, and circular craniotomies with a diameter of 0.9 mm were made with a high-speed drill (SD-102, Narishige, Tokyo, Japan) at co-ordinates of 0.3 mm posterior and 1.9 mm bilateral to the bregma for the motor cortex and 10.0 mm anterior and 0.2–0.5 mm bilateral to the bregma for the olfactory bulb (OB). Stainless-steel screw-shaped LFP electrodes were implanted on the surface of these craniotomies. In addition, stainless-steel screws were implanted on the surface of the cerebellum (9.6 mm posterior and 0.8–1.0 mm bilateral to the bregma) as earth/reference electrodes. Finally, the open edges of the LFP, ECG, EMG, VN and earth/reference electrodes were soldered to the open edges of the insulated wires protruding from the corresponding channels on the EIB. All the wires and the electrode assembly were secured to the skull using dental cement. After all the electrodes had been affixed to the animals' heads, the animals were allowed to recover from anaesthesia.

Post-operative monitoring

Following surgery, each animal was housed in a transparent Plexiglas cage with free access to food and clean water (or gelled water; HydroGel, ClearH2O, Portland, ME, USA) both on its flooring and above the cage. For the first 2 days after surgery, the animals were carefully checked every 3 h except during the night (from 20.00 to 08.00 h). After this time they were checked with an interval of <6 h at least 3 times per day. While our experimental protocols have a mandate to humanely kill animals if they exhibit any signs of pain, prominent lethargy and discomfort, we did not observe such symptoms in any of the 13 rats used in this study. In addition, we continuously monitored the animals' body weight every day and verified that changes in body weight in individual animals were restricted to less than 20 g (less than 5%) from the beginning of surgery to the recording day, indicating that the animals were normally feeding and drinking. The average weight before and after surgery on the recording day was (mean ± SEM) 348.0 ± 9.6 g (range 296–400 g) and 347.7 ± 8.9 g (range 310–390 g), respectively. Electrophysiological recordings commenced more than 5 days (range 5–9 days) after the surgery. During recordings, the animal's behaviour and health were monitored by a video camera on the ceiling.

Electrophysiological recordings

For electrophysiological recording, the EIB of the electrode assembly was connected to a Cereplex M digital headstage (Blackrock Microsystems, Salt Lake City, UT, USA), and the digitized signals were transferred to a Cereplex Direct data acquisition system (Blackrock Microsystems). LFP, ECG and EMG signals were recorded at a sampling rate of 2 kHz, and VN signals were recorded at a sampling rate of 30 kHz.

Recordings in a home cage, open field and elevated plus maze

Recordings were taken from Sprague–Dawley rats. All behavioural tests occurred between 09.00 and 17.00 h, which was during the dark phase of the rats' inverted light/dark cycle. The animals were not handled at all before the start of the following procedures. One day before behavioural tests, the animals were first placed in a transparent rest box (22 cm × 38 cm) with a wall height of 20 cm at least once for up to 30 min. The rest box was at least 2 m distant from the recording setups and a barrier wall was in place so that the rats in the rest box could not directly see the open field and the elevated plus maze. On the recording day, the rats were habituated in the same rest box for 2 h, after which electrophysiological recording started in the rest box. Throughout these habituation periods 1 day before and on the recording day, the rats were connected to the headstage to habituate them to tethering.

For recordings in a novel open field, each rat was placed individually in an open field (75 cm × 75 cm) with a wall height of 50 cm and allowed to move freely throughout the field for 10 min. The floor was illuminated with an overhead light, which produced a light intensity of 25 lx in the field.

For recordings in a novel elevated plus maze, the rat was placed on the central square facing one of the open arms and allowed to freely explore the maze apparatus for 10 min. The elevated plus maze was made of ABS resin and consisted of a central square (10 cm × 10 cm) and four arms (50 cm long × 10 cm wide, two open arms with no railing and two closed arms enclosed by vertical walls

40 cm in height). The maze was elevated 88.5 cm from the floor and illuminated with four 32 W fluorescent overhead lights, which produced light intensities of 480 lx and 40 lx in the open and closed arms, respectively.

For all recordings, LED reflection tape (1 cm × 1 cm) was attached to the outer cover of the electrode assembly, and the position of the LED signal was tracked at 15 Hz using an infrared video camera attached to the ceiling; the data were sampled with a laptop computer. The rat's moment-to-moment position was automatically detected from the LED reflection tape by setting a threshold of light intensity. Rearing behaviour was manually detected by eye.

Social defeat stress

Recordings were taken from Long Evans rats. A recording day for each rat consisted of three sessions: a 30 min pretest session in a rest box (24 cm × 40 cm × 35 cm), a stress session of up to 10 min in an open field (50 cm × 50 cm × 60 cm) and a 120 min post-test session in the same rest box. Acute stress was applied to the recorded rat as in rat resident–intruder tests (Sgoifo *et al.* 1997; Marini *et al.* 2006). To prepare an experimental environment for the stress session, we housed a male and a female rat as resident rats in the open field for at least 1 h per day for 7 days before the stress session. At the beginning of the stress session, the female resident rat was removed from the field, and the recorded rat was placed in the open field as an intruder rat. During the stress session, the intruding recorded rat was physically attacked by the resident male rat for 10 min. While our experimental protocols have a mandate that the social defeat stress session is immediately terminated if rats are wounded and bleeding due to the attack, we did not observe such symptoms in any of the three intruder rats and two resident rats during the 10 min stress session in this study. Before social defeat stress, the resident male rats were selected based on the observations that they had attack latencies shorter than 60 s when they were exposed to several rats that were not used for the subsequent experiments.

Data analysis

Any signal that included apparent electrical noise due to physical collisions of the animal's head with the walls or the resident rats were manually removed. All of the following factors were computed in each 1 s bin. Cortical LFP traces were convolved using a Morlet wavelet family, and the power of the delta (2–4 Hz) and theta (6–10 Hz) bands was computed. OB LFP traces were convolved using a Morlet wavelet family, and the power spectrum was processed with a Gaussian filter ($\sigma = 5$ s). The ratio of 6–9 Hz power to 1–4 Hz power was computed as the sniff ratio. In the spectrum, the frequencies ($Freq_{max}$) giving the maximum power within the frequency band, with an upper limit of 10 Hz, were computed. Time bins with a $Freq_{max}$ of less than 1 Hz or more than 9 Hz were considered bins in which the sniff rate was not precisely estimated and were excluded from further analyses (e.g. 5–10 s in Fig. 1*B* Example 1). In the other bins, if the sniff ratios were less than 1, instantaneous sniff rates were defined as the frequencies giving the maximum power within the frequency band of 1–4 Hz. If the sniff ratios were greater than 1, instantaneous sniff rates were defined as the frequencies giving the maximum power within the frequency band of 6–9 Hz. Sniff rates of 1–4 Hz and >6 Hz were considered resting respiration (RR) and HF sniffing, respectively. ECG signals were bandpass filtered at 20–200 Hz, and beat-to-beat intervals (R–R intervals) were calculated from the timestamp of the R-wave peak. Instantaneous heart rates were computed by averaging the R–R intervals. EMG traces were high-pass filtered at 100 Hz, and root mean square (rms) values were calculated from the filtered EMG traces, which were used to represent the absolute changes in EMG amplitude and define the animal's arousal state. For VN signals, a spike unit was detected when the amplitude of a negative deflection of the extracellularly recorded signals exceeded a threshold of 7–20 μV, which corresponded to five standard deviations from the baseline of the VN signals recorded during quiescent periods in individual animals. Burst spike units detected within a 10 ms bin were regarded as a single spike (Shikano *et al.* 2019).

All analyses were performed in MATLAB (MathWorks, Natick, MA, USA). Comparisons of two-sample data were analysed by Student's *t* test or, if the data did not meet the assumptions of the Student's *t* test, they were analysed with the non-parametric Mann–Whitney *U* test. Where the numbers of samples did not match between the two groups, as in the cases where two out of five rats never showed 'stop-high frequency (HF) sniffing' periods, resulting in $n = 3$ samples at 'stop-HF sniffing' in Figs 4*C* and *E*, 5*G* and 6*C*, they were analysed with the non-parametric Mann–Whitney *U* test. Multiple groups were compared with individual tests followed by *post hoc* Bonferroni corrections. The null hypothesis was rejected at the $p < 0.05$ level unless otherwise specified. All data are presented as the mean ± standard error of the mean (SEM).

Results

Detection of sniffing rates based on OB LFP signals

Bioelectrical signals were recorded from the brain and peripheral organs of freely moving rats, including LFP signals from the motor cortex (Cor LFP) and the olfactory bulb (OB LFP), an ECG signal, a dorsal neck muscle EMG signal, and a signal from the left cervical VN (Fig. 1*A* and *B*). OB LFP traces were convolved to a power spectrogram,

and instantaneous sniff rates were computed within a range of 1–9 Hz, as represented by the cyan dots (Fig. 1*C*; for more detail, see Methods). On the basis of the bimodal distribution of sniff rates, peaking at 2.5 and 8.9 Hz, two distinct periods were identified: (1) resting respiration (RR) at a sniff rate of 1–4 Hz and (2) HF sniffing at a sniff rate of >6 Hz (Fig. 1*B* and *C*) (Wesson, 2013; Tsanov *et al.* 2014; Sasaki *et al.* 2017). Some periods that did not meet the criteria were excluded from further analyses (e.g. 5–10 s in Fig. 1*C* Exp 1). On average, sniff rates during RR and HF sniffing were 2.4 and 7.9 Hz, respectively. Figure 1*C* Exp 1 and 2 illustrates typical cases in which the rats showed an abrupt transition from RR to sustained HF sniffing, whereas Exp 3 shows a case in which the rat rapidly changed from HF to RR.

HF sniffing in a novel open field

The rats were tested in a familiar home cage and a novel open field (Fig. 2*A*). Overall, instantaneous moving speed (bin = 1 s) in the open field was higher than that in the home cage (Fig. 2*B*; $n = 5$ rats, $D_{max} = 0.39$, $P < 10^{-99}$, Kolmogorov–Smirnov test). Here, frames at a speed of more than 10 cm s^{-1}, between 3 and 10 cm s^{-1}, and less than 3 cm s^{-1} were classified as fast, slow and stop periods, respectively. Slow periods contained a mixture of behavioural patterns such as acceleration, deceleration, grooming, rearing and swinging. In the home cage, no fast periods were detected due to the limited size of the cage. Figure 2*C* shows example datasets depicting the animals' behavioural patterns, running speed and OB LFP spectra observed in a familiar home cage and a novel open field. To confirm how sniffing behaviour depends on the animal's locomotion, we plotted sniff rates against the instantaneous moving speed of animals (Fig. 2*D* and *E*; $n = 5$ rats in each condition). During the stop periods in the home cage, the rats exhibited HF sniffing for 9.3 ± 5.1% of the entire periods (Fig. 2*D*, $n = 5$ rats). In the open field, fast frames composed 6.8 ± 3.0% of the entire recording period (Fig. 2*E*). The majority (97.2 ± 2.0%) of such fast frames included HF sniffing. However, there were several cases in which HF sniffing did not emerge during a fast period, as shown in Fig. 2*F* Exp 3. During stop periods in the open field, the rats exhibited HF sniffing in 20.8 ± 9.4% of the stop periods. Based on these data, individual periods were subdivided into HF sniffing and RR periods depending on the presence of HF sniffing. Overall, the percentage of HF sniffing was significantly higher in the novel open field than in the home cage (Fig. 2*D* and *E*; $n = 5$ rats, $t_4 = 2.98$, $P = 0.041$, paired *t* test), confirming the idea that HF sniffing emerges

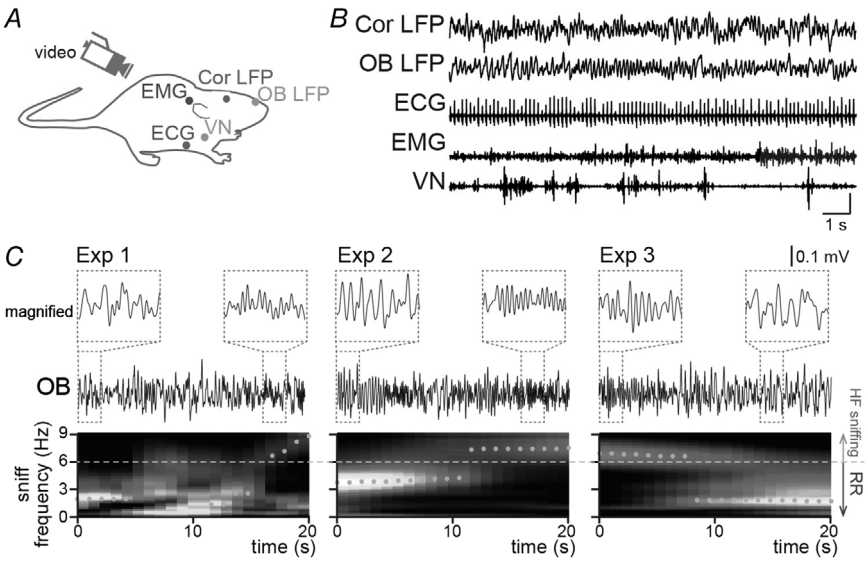

Figure 1. Calculation of olfactory bulb (OB)-based sniff rates and detection of high-frequency (HF) sniffing in rats
A, schematic illustration of the recordings. *B*, representative electrophysiological recordings of a motor cortex local field potential (LFP) signal (Cor LFP, red), an OB-based LFP signal (OB LFP, orange), a 20–100 Hz filtered ECG signal (magenta), a dorsal neck muscle EMG signal (blue), and a 500–1000 Hz filtered vagus nerve (VN) signal (green). The vertical scale bar represents 1 mV (LFP and ECG) and 0.1 mV (EMG and VN). *C*, three representative examples showing abrupt changes in sniff rates. Individual OB LFP traces were converted to the colour-coded power spectrum shown below. Dotted boxes are magnified above. In each frame on the spectrum, the frequencies giving the maximum power were detected as instantaneous sniff rates, as indicated by the cyan dots. Periods with a sniff rate of more than 6 Hz were considered HF sniffing.

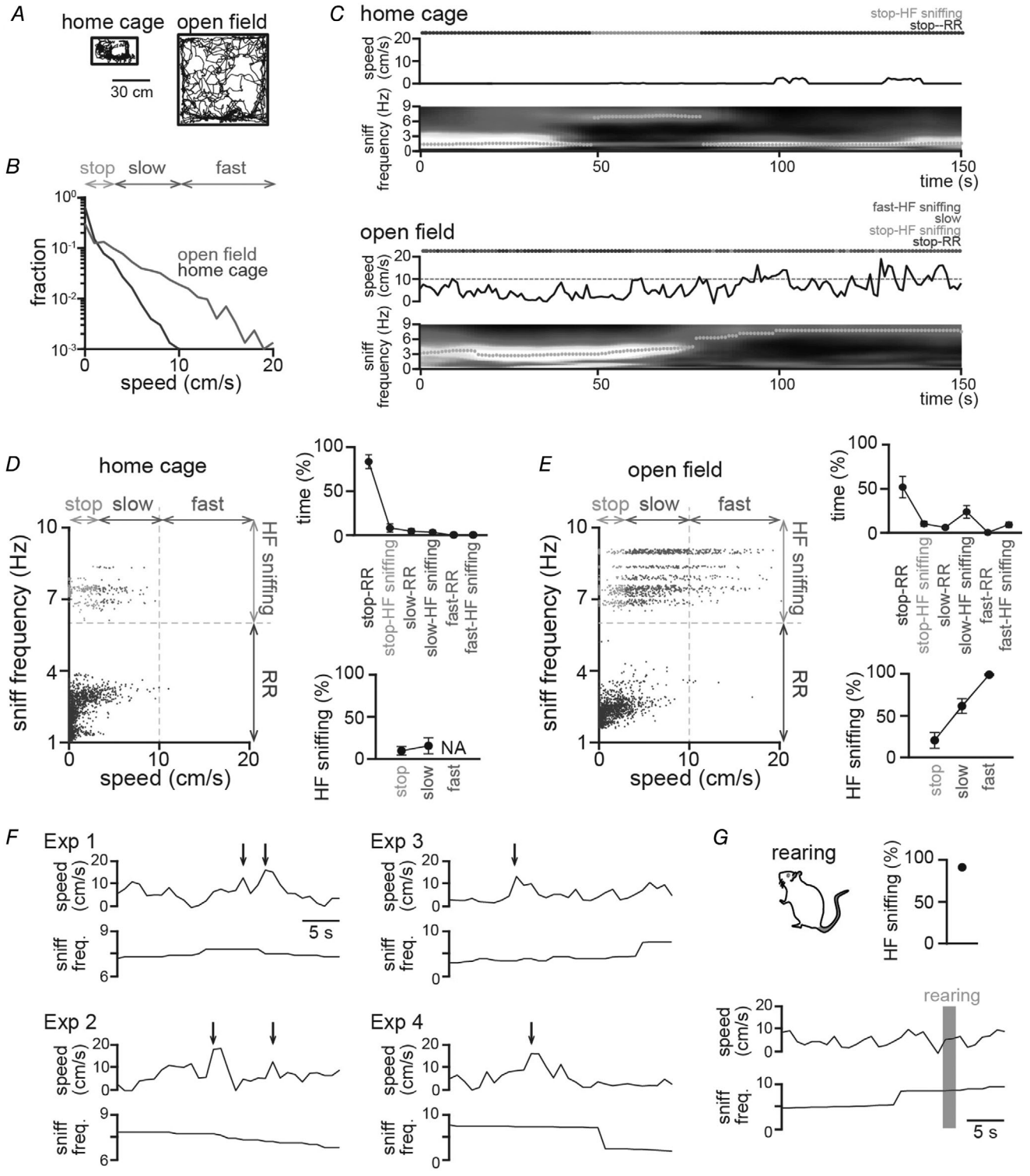

Figure 2. Emergence of HF sniffing in familiar and novel contexts
A, representative 10 min moving trajectories of a rat in a familiar home cage and a novel open field. *B*, distribution of instantaneous moving speed (bin = 1 s). Fast, slow and stop periods were defined based on instantaneous moving speed. *C*, from top to bottom, time-dependent changes in behavioural patterns (indicated by coloured dots), instantaneous running speed and the colour-coded OB LFP power spectrum with cyan dots showing sniff rates. *D*, left, plots of sniff rates against animals' moving speed in each 1 s frame observed in the home cage. Based on the parameters, each frame was classified as fast-HF sniffing (magenta), slow behaviour (dark green), stop-HF sniffing (light green), or stop-resting respiration (RR) (blue) periods. The horizontal and vertical dotted

more frequently and animals are more strongly motivated to explore in a novel and/or open environment than in a closed, familiar environment such as the home cage (Clarke & Trowill, 1971).

We further characterized the relationship between moving speed and HF sniffing. A speed–sniff rate correlation restricted within fast periods, which corresponded with the plots at >10 cm s^{-1} in Fig. 2*E*, was not significant ($r = 0.024$, $P = 0.74$), implying that sniff rates during HF sniffing are not strongly dependent on running speed. Figure 2*F* presents four typical cases in which transient increases in running speed occurred, as indicated by the arrows, but they were not associated with apparent changes in sniff rates during HF sniffing. These results verify that sniff rates during HF sniffing are not simply determined by running speed.

The other behavioural pattern associated with sniffing behaviour is rearing (Kurnikova *et al.* 2017) (Fig. 2*G*). Over the course of 10 min in the open field, two out of five rats showed rearing behaviour with a duration of up to 3 s during slow periods, in which one mouse reared 5 times and the other mouse reared 3 times, resulting in a total of 8 rearing periods. Consistent with the previous report (Kurnikova *et al.* 2017), HF sniffing was detected in most of these rearing periods ($n = 7$ times).

HF sniffing is related to emotional changes

We tested how HF sniffing events are affected by emotional changes using an additional four rats on a novel elevated plus maze with two open and two closed arms (Fig. 3*A*). In these experiments, fast periods (1.5 ± 0.6% of entire recording periods) were rarely detected in both of the arms and such periods were thus excluded from our analysis. In stop and slow periods, the percentage of stop-HF sniffing was significantly higher in open arms than in closed arms ($n = 4$ rats, $t_3 = 3.69$, $P = 0.034$, paired t test), which demonstrates that the duration of HF sniffing events is increased in open environments as well as the novel open field.

We examined how sniffing is affected by stress experiences. Three Long Evans rats were subjected to social defeat stress by a resident rat for 10 min. The rat was placed in the rest box for 20 min before and 20 min after the stress session; these recording conditions were termed 'before stress' and 'after stress', respectively. After stress exposure, the percentage of the entire time spent in HF sniffing was significantly decreased (Fig. 3*B*, bottom right; $n = 3$ rats, $t_2 = 9.50$, $P = 0.011$, paired t test) and instantaneous moving speed was significantly lowered (Fig. 3*B*, bottom left; $n = 3$ rats, $D_{max} = 0.18$, $P = 5.5 \times 10^{-49}$, Kolmogorov–Smirnov test). The concurrent decreases in running speed and HF sniffing might imply that the stress-associated decreases in HF sniffing were simply accounted for by the reduction in locomotor activity. This possibility was unlikely because the stress-related decrease in HF sniffing was still detected even when HF sniffing was quantified within the same speed range; the percentage of time spent in HF sniffing during slow speed in the after stress condition (24.4 ± 9.3%) was significantly lower than that in the before stress condition (31.4 ± 10.5%) (Fig. 3*B*, top right; $n = 3$ rats, $t_2 = 4.54$, $P = 0.045$, paired t test). These results demonstrate that the decreased moving speed alone could not explain the reduction in HF sniffing after experiencing stressful episodes. Therefore, the stress-induced reduction in HF sniffing is mainly induced by changes in internal emotional states.

HF sniffing-related changes in peripheral physiological activity

We examined how systemic physiological signals are changed in relation to HF sniffing. In subsequent analyses, we excluded slow periods as they contained complex behavioural patterns. For individual behavioural patterns, instantaneous heart rates and the root mean square (rms) of dorsal neck muscle EMG signals with and without HF sniffing were plotted against moving speed (Fig. 4*A*, *B* and *D*). Both signals in the open field showed significant positive correlations with moving speed ($n = 5$ rats, heart rate, $r = 0.43$, $P = 2.8 \times 10^{-115}$; EMG rms, $r = 0.65$, $P = 2.7 \times 10^{-306}$). Notably, the majority of points with stop-HF sniffing (green dots) were located above the linear regression lines, as shown in Fig. 4*B* and *D*, which demonstrates that physiological activity during stop-HF sniffing periods was markedly higher than expected from the simple linear regressions. Indeed, statistical analyses verified that heart rates were significantly higher during stop-HF sniffing periods than during stop-RR periods (Fig. 4*C*; $n = 5$ rats, $t_4 = 2.90$, $P = 0.044$, paired t test), whereas such differences were not observed in the home cage ($U = 20$, $P = 0.57$, Mann–Whitney U test). No significant differences in heart rates were found between stop-HF sniffing or stop-RR periods in

lines represent 6 Hz and 10 cm s^{-1}, respectively. Right top, average durations of behaviours as percentages of the overall recording periods in the home cage ($n = 5$ rats). Right bottom, the overall percentages of HF sniffing time within the fast, slow and stop periods. A value was described as N/A if fast periods were not detected. *E*, same as in *D* but for the novel open field ($n = 5$ rats). *F*, four representative cases showing temporal changes in moving speed and sniff rates. The arrows indicate transient increases in moving speed exceeding 10 cm s^{-1}. *G*, top, the percentage of HF sniffing during rearing behaviour ($n = 8$ rearing from 2 rats). Bottom, representative case including rearing behaviour as labelled by the green area.

the home cage and stop-RR periods in the open field (stop-HF sniffing: $U = 13$, $P = 1.00$, Mann–Whitney U test followed by Bonferroni correction; stop-RR: $U = 20$, $P = 0.30$, Mann–Whitney U test followed by Bonferroni correction). The same statistical results were observed for the rms values of EMG signals; these values were significantly higher during stop-HF sniffing periods than during stop-RR periods in the open field (Fig. 4*E*; $n = 5$ rats, $t_4 = 3.89$, $P = 0.018$, paired t test) but not in the home cage ($U = 25$, $P = 0.57$, Mann–Whitney U test), and there were no significant differences between stop-HF sniffing or stop-RR periods in the home cage and stop-RR periods in the open field (stop-HF sniffing: $U = 11$, $P > 0.99$, Mann–Whitney U test followed by Bonferroni correction; stop-RR: $U = 25$, $P > 0.99$, Mann–Whitney U test followed by Bonferroni correction).

The results above showed that heart rates and EMG amplitude during stop-HF sniffing in the open field were higher than those in the home cage (Fig. 4*C*, ECG: $U = 6$, $P = 0.0035$; Fig. 4*E*, EMG: $U = 8$, $P = 0.14$; Mann–Whitney U test). These increases in peripheral activity might be explained by increased locomotion in the open field (Fig. 2*B*). In particular, post-running effects on peripheral activity might be sustained for a certain period of time after running. To test this possibility, we classified stop periods into two types (Fig. 4*F*); (1) post-run stop periods defined as stop periods up to 20 s after the offset of slow and fast periods, and (2) long-lasting stop periods defined as the other stop periods. The percentage of HF sniffing during post-run stop periods was 78.4 ± 10.4%, which was prominently higher than that during long-lasting stop periods (7.1 ± 3.1%) (Fig. 4*G*). However, no significant differences in either heart rates or EMG amplitude were found between post-run stop periods and long-lasting stop periods (Fig. 4*H*; $U = 19$, $P = 0.90$; EMG, $U = 21$, $P = 0.90$; Mann–Whitney U test). These results demonstrate that post-run periods, in which the frequency of HF sniffing become prominently higher, do not account for peripheral activity. Possibly, changes in internal emotional states in the open field might underlie the overall increases in peripheral activity levels. Taken together, these results suggest that HF sniffing-induced increases in heart rates and neck muscle contraction during stop periods were prominent in novel and/or open environments.

Next, we examined spike patterns from a fibre bundle of the VNs. We first computed an autocorrelation of VN spikes to test whether they had typical temporal patterns (Fig. 5*A* and *C*). In all five animals tested, no prominent peaks in their autocorrelograms were detected within a temporal range of both 1 s and 10 s, revealing no apparent temporal patterns in the spike trains of the VNs. We then tested whether temporal changes in VN spike rates are correlated to instantaneous running speed and heart rates by computing their crosscorrelograms (Fig. 5*B* and *D*). No apparent temporal structures were detected in the correlograms of all five animals tested, demonstrating that VN spikes were not tightly associated with instantaneous running speed and heart rates.

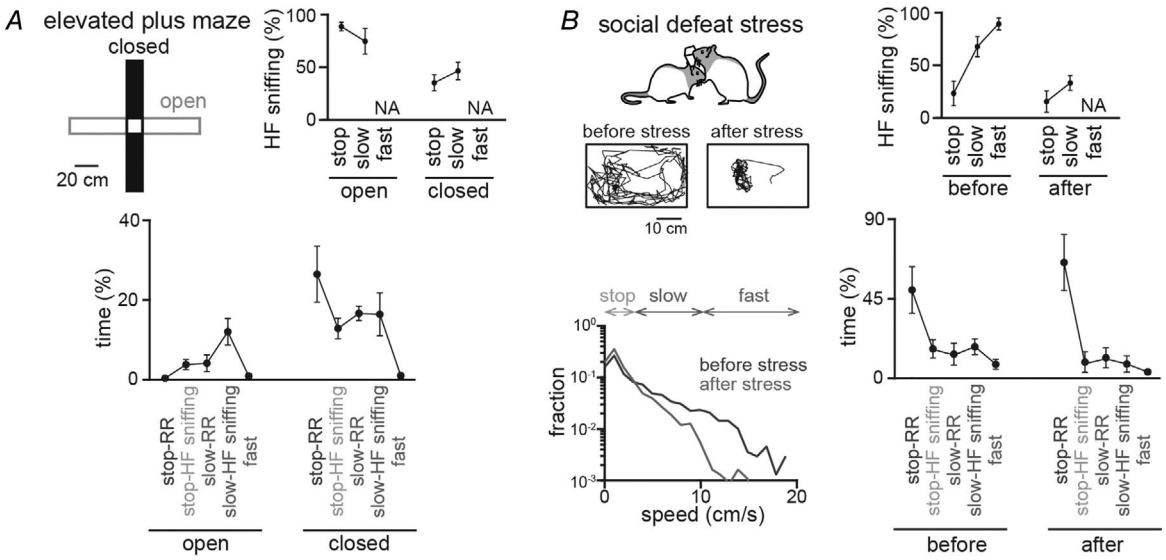

Figure 3. Emotion-related changes in moving speed and HF sniffing
A, same as in Fig. 2*D* but for the data from an elevated plus maze. Top, changes in the average percentages of time spent on HF sniffing, separately analysed for the open and closed arms of the elevated plus maze ($n = 5$ rats). Bottom, average percentages of time spent in different behaviours. *B*, effects of social defeat stress on sniffing behaviour. Top left, representative 5 min moving trajectories of a rat before and after social defeat stress. Bottom left, distribution of instantaneous moving speed before and after social defeat stress (bin = 1 s) ($n = 3$ rats). Right, same as in *A* but for periods before and after social defeat stress.

With the same analytical approach to Fig. 4, we next tested how sniffing is related to VN spike rates (Fig. 5*E* and *F*). The overall average VN spike rates were higher in the open field than in the home cage (Fig. 5*G*; $n = 5$ rats, $t_4 = 2.89$, $P = 0.044$, paired *t* test). However, no significant differences in VN spike rates were found between periods with and without HF sniffing in either condition ($n = 5$ rats, home cage: $U = 12$, $P = 0.79$, Mann–Whitney *U* test; open field: $F_{(2,12)} = 1.50$, $P = 0.26$, one-way ANOVA). These results imply that HF sniffing does not have a pronounced impact on VN spike activity.

Sniffing-associated changes in cortical arousal states

Cortical LFP signals represent the neuronal activity of the nearby neuronal population, including spiking and neurotransmission, and these signals can reflect a variety of cognitive processes. We examined how changes in sniffing rates affect the LFP power of the motor cortex, especially for the ratio of LFP theta (θ, 6–10 Hz) to delta (δ, 2–4 Hz) power (Fig. 6), which has conventionally been used to define animal arousal/sleep levels (Vyazovskiy *et al.* 2009; Watson *et al.* 2016). In both the home cage and the open field, LFP θ/δ ratios during stop periods were significantly elevated when the rats exhibited HF sniffing (Fig. 6*C*; $n = 5$ rats, home cage: $U = 15$, $P = 0.036$, Mann–Whitney *U* test; open field: $t_4 = 7.94$, $P = 0.0028$, paired *t* test followed by Bonferroni correction). In the open field, HF sniffing-related LFP θ/δ ratios were not significantly different between move and stop periods ($n = 5$ rats, $t_4 = 2.55$, $P = 0.13$, paired *t* test followed by Bonferroni correction), and the same was true of heart rates and the rms of EMG signals. These results

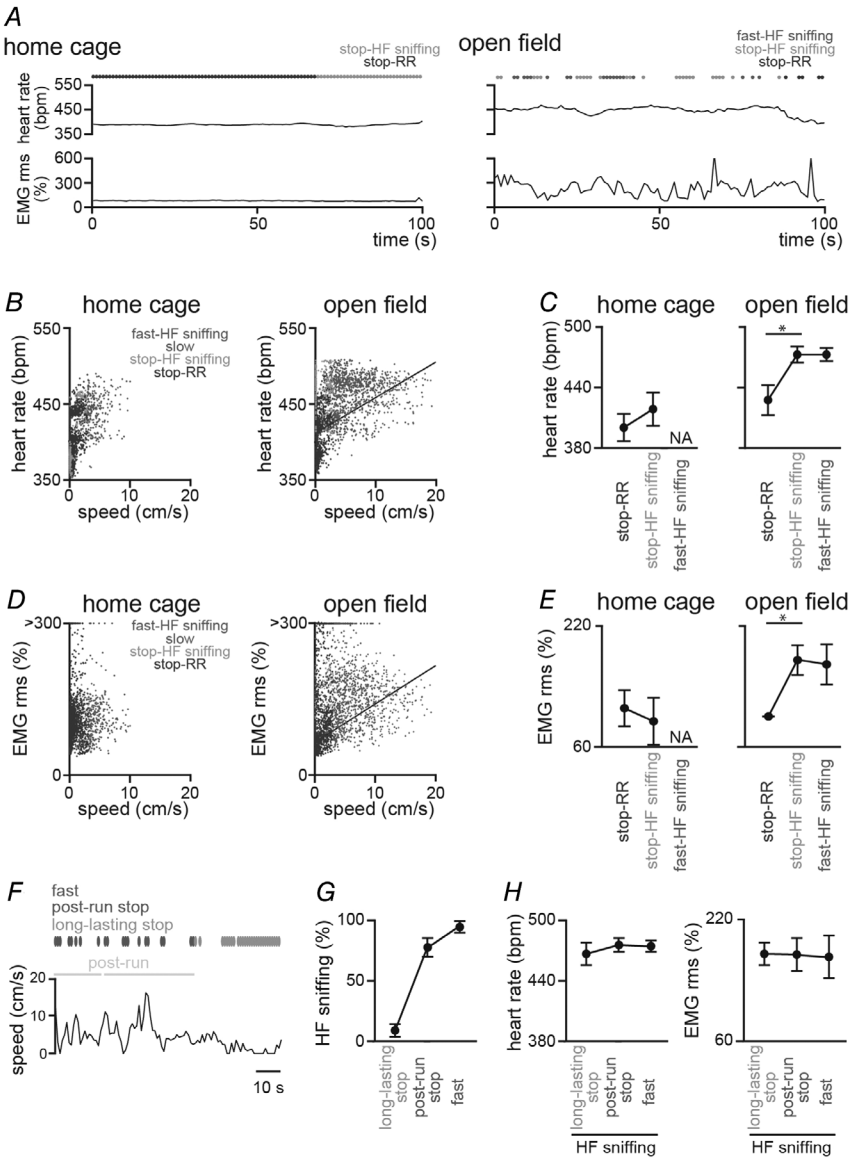

Figure 4. Heart rates and EMG amplitudes during sniffing
A, from top to bottom, time-dependent changes in behavioural patterns (as indicated by coloured dots), instantaneous heart rates, and the rms of EMG. *B* and *D*, plotting individual instantaneous heart rates (*B*) and the rms of EMG (*D*) against moving speed in each frame ($n = 5$ rats). The linear regression lines are shown ($n = 5$ rats, heart rates, $r = 0.43$, $P = 2.8 \times 10^{-115}$; EMG rms, $r = 0.65$, $P = 2.7 \times 10^{-306}$). *C* and *E*, average heart rates and the rms of EMG signals averaged over individual behavioural periods. *F*, classification of running-related periods. A representative temporal change in moving speed. Periods 0–20 s after the offset of fast/slow periods were considered as post-run periods (yellow). Fast, post-run stop, and long-lasting stop periods were indicated by upper coloured dots. *G*, the percentage of time spent on HF sniffing during individual behavioural patterns. *H*, same as in *C* and *E* but for post-run stop and long-lasting stop periods. $^*P < 0.05$.

demonstrate that increases in LFP θ/δ ratios during HF sniffing were equivalent between move and stop periods.

Discussion

By utilizing the unique ability of OB LFP signals to reflect sniffing cycles, we classified rat sniffing patterns into two modes: RR at a sniff rate of 1–4 Hz and HF sniffing at a sniff rate of >6 Hz. We then analysed how ongoing changes in sniffing patterns were associated with changes in brain and peripheral physiological signals that have been widely utilized as objective measures to gauge animal psychological states and arousal/sleep states, including cortical LFP, ECG and EMG signals. Our physiological data will help clarify how these factors undergo dynamic changes depending on sniffing patterns.

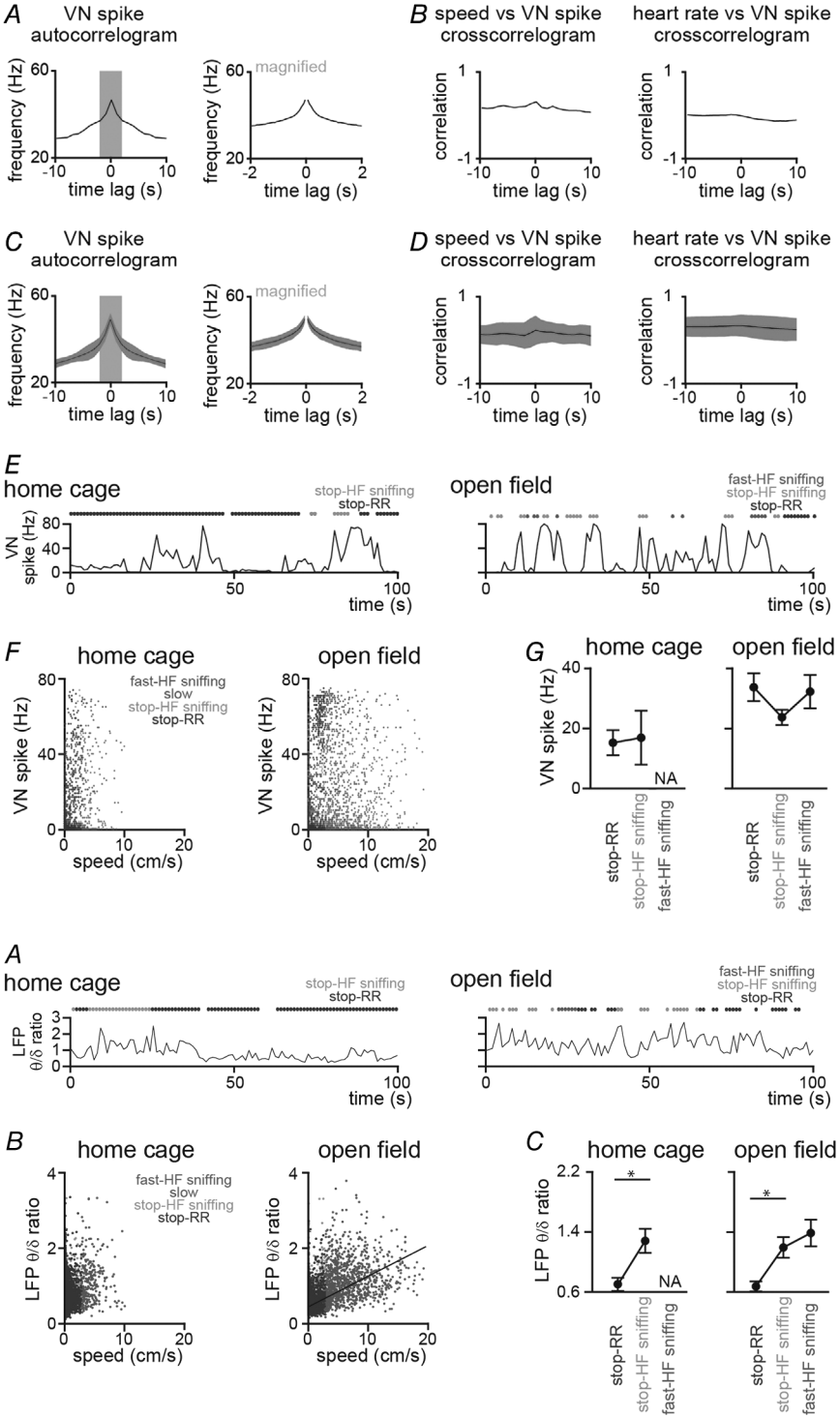

Figure 5. VN spikes during sniffing
A, VN spike–time autocorrelogram for a single rat. The green area (−2 to 2 s) is magnified in the right panel. *B*, left, crosscorrelogram of temporal changes between instantaneous running speed and VN spike rates (bin = 1 s) for a single rat. Right, crosscorrelogram between instantaneous heart rates and VN spike rates. *C* and *D*, same as in *A* and *B*, respectively, but for averaged data from 5 rats. Black lines and shaded regions represent mean and standard deviation, respectively. *E*, from top to bottom, behavioural patterns (as indicated by coloured dots) and VN spike rates, plotted as in Fig. 3*A*. *F*, same as in Fig. 3*B* but plotted for VN spike rates. *G*, VN spike rates averaged over individual behavioural periods ($n = 5$ rats).

Figure 6. Cortical LFP theta/delta ratio during sniffing
A, from top to bottom, behavioural patterns (as indicated by coloured dots) and the ratios of theta (θ, 6–10 Hz) to delta (δ, 2–4 Hz) somatosensory cortical LFP power, termed LFP θ/δ ratios. *B*, same as in Fig. 3*B* but plotted for LFP θ/δ ratios. The linear regression line is shown ($n = 5$ rats, $r = 0.39$, $P = 8.9 \times 10^{-108}$). *C*, LFP θ/δ ratios averaged over individual behavioural periods ($n = 5$ rats). $^*P < 0.05$.

HF sniffing was observed in a novel environment but not in a familiar home cage. Notably, the majority of fast periods (>10 cm s^{-1}) included HF sniffing whereas stop periods intermittently included HF sniffing, with the other periods accounted for by RR. In the majority of previous studies (Uchida & Mainen, 2003; Kepecs *et al.* 2007; Verhagen *et al.* 2007; Tsanov *et al.* 2014), this speed–HF sniffing relationship has been not tested because animals tested in these studies did not move with such fast speed. We cannot exclude a possibility that the speed–HF sniffing relationship is specific to our experimental conditions. Further studies are required to determine whether this relationship is applicable to the other behavioural contexts.

The percentage of HF sniffing was higher in a novel open field and an elevated plus maze than in a familiar home cage, suggesting that HF sniffing by rodents is induced by both the openness and the novelty of the environment. Furthermore, the percentage of HF sniffing in the elevated plus maze was significantly higher in the open environment than in the closed environment. Based on the fundamental premise that time spent in the open arms in an elevated plus maze test evaluates anxiety and/or motivation levels of rodent animals (Handley & Mithani, 1984; Walf & Frye, 2007; Komada *et al.* 2008; Schneider *et al.* 2011; Okonogi *et al.* 2018), we suggest that HF sniffing is highly sensitive to changes in these internal psychiatric states. In addition, we demonstrated that rats exhibited reduced HF sniffing after being exposed to social defeat stress. Generally, when animals experience severe stressful episodes and threats, they become more conservative and less motivated to explore external environments. Such instinctive behavioural habits are consistent with our observations of stress-induced decreases in HF sniffing.

Instantaneous heartbeat, muscle contraction and cortical LFP signals rapidly change with locomotor activity, as shown by their correlation with speed of movement. However, we showed that some activity levels during stop periods were higher than those expected from a simple linear correlation. This supralinear relationship was mainly explained by the presence of HF sniffing, which led to peripheral activity levels during stop-HF sniffing that were equivalent to those during move periods. These results demonstrate that the physiological signals in stop periods are not homogeneous and suggest that the presence of sniffing during stop periods may be one of the crucial factors influencing these physiological signals.

Using a new recording method that can monitor the spike pattern of the VN fibres by means of a cuff-shaped electrode, we revealed that the frequency of VN spikes was higher in novel conditions than in familiar conditions (Shikano *et al.* 2019). In addition to this finding, this study showed that there were no prominent differences in the frequency of VN spikes between HF sniffing and RR. This result appears at odds with our observation that other peripheral organ activity, such as heartbeats and dorsal neck muscle contraction, was rapidly altered in synchrony with changes in sniff rates. A possible explanation for this seeming contradiction is that the novelty- and openness-induced peripheral activity may be mainly transmitted via visceral sensory nerves other than the VN. The other possibility is that, as sniffing is a behaviour mainly controlled by the central nervous system, there might be no need to transfer signals to the peripheral organs through the VN during HF sniffing.

To evaluate psychological function and understand the physiological activity patterns of the peripheral organs, studies have analysed several major factors in rodents, including apparent behavioural patterns. In addition to these behavioural patterns, animals frequently exhibit rapid bouts of nasal inhalation, represented as transient increases in sniffing frequency. While sniffing patterns are considered to reflect an animal's motivation for exploration, it remains to be fully clarified how they undergo changes during observable emotion-related behavioural patterns. Moreover, little is known about how such sniffing behaviour affects the physiological activity of the brain–body system. In this study, we have demonstrated pronounced sniffing-related increases in a variety of central and peripheral physiological organ activities as opposed to a simple relationship with body movement. The results suggest that sniffing can be a physiological marker, in addition to behavioural tests, that enables us to more accurately evaluate physiological states in the central and peripheral systems in rodents.

References

Brankack J & Klingberg F (1982). Behaviour-dependent changes of visually evoked potentials and their correlation to the respiration rate in freely moving rats. *Acta Biol Med Ger* **41**, 315–324.

Carlson KS, Dillione MR & Wesson DW (2014). Odor- and state-dependent olfactory tubercle local field potential dynamics in awake rats. *J Neurophysiol* **111**, 2109–2123.

Cheung MC, Carey RM & Wachowiak M (2009). A method for generating natural and user-defined sniffing patterns in anesthetized or reduced preparations. *Chem Senses* **34**, 63–76.

Clarke S, Panksepp J, Trowill J & Pankseep J (1970). A method of recording sniffing in the free-moving rat. *Physiol Behav* **5**, 125–126.

Clarke S & Trowill JA (1971). Sniffing and motivated behavior in the rat. *Physiol Behav* **6**, 49–52.

Grundy D (2015). Principles and standards for reporting animal experiments in *The Journal of Physiology* and *Experimental Physiology*. *J Physiol* **593**, 2547–2549.

Handley SL & Mithani S (1984). Effects of alpha-adrenoceptor agonists and antagonists in a maze-exploration model of 'fear'-motivated behaviour. *Naunyn Schmiedebergs Arch Pharmacol* **327**, 1–5.

Hayashi Y, Kashiwagi M, Yasuda K, Ando R, Kanuka M, Sakai K & Itohara S (2015). Cells of a common developmental origin regulate REM/non-REM sleep and wakefulness in mice. *Science* **350**, 957–961.
Jessberger J, Zhong W, Brankack J & Draguhn A (2016). Olfactory bulb field potentials and respiration in sleep-wake states of mice. *Neural Plast* **2016**, 4570831.
Kepecs A, Uchida N & Mainen ZF (2007). Rapid and precise control of sniffing during olfactory discrimination in rats. *J Neurophysiol* **98**, 205–213.
Komada M, Takao K & Miyakawa T (2008). Elevated plus maze for mice. *J Vis Exp* https://doi.org/10.3791/1088.
Kurnikova A, Moore JD, Liao SM, Deschenes M & Kleinfeld D (2017). Coordination of orofacial motor actions into exploratory behavior by rat. *Curr Biol* **27**, 688–696.
Marini F, Pozzato C, Andreetta V, Jansson B, Arban R, Domenici E & Carboni L (2006). Single exposure to social defeat increases corticotropin-releasing factor and glucocorticoid receptor mRNA expression in rat hippocampus. *Brain Res* **1067**, 25–35.
Oishi Y, Takata Y, Taguchi Y, Kohtoh S, Urade Y & Lazarus M (2016). Polygraphic recording procedure for measuring sleep in mice. *J Vis Exp* **25**, e53678.
Okada S, Igata H, Sakaguchi T, Sasaki T & Ikegaya Y (2016). A new device for the simultaneous recording of cerebral, cardiac, and muscular electrical activity in freely moving rodents. *J Pharmacol Sci* **132**, 105–108.
Okonogi T, Nakayama R, Sasaki T & Ikegaya Y (2018). Characterization of peripheral activity states and cortical local field potentials of mice in an elevated plus Maze test. *Front Behav Neurosci* **12**, 62.
Rojas-Libano D, Frederick DE, Egana JI & Kay LM (2014). The olfactory bulb theta rhythm follows all frequencies of diaphragmatic respiration in the freely behaving rat. *Front Behav Neurosci* **8**, 214.
Sasaki T, Nishimura Y & Ikegaya Y (2017). Simultaneous recordings of central and peripheral bioelectrical signals in a freely moving rodent. *Biol Pharm Bull* **40**, 711–715.
Schneider P, Ho YJ, Spanagel R & Pawlak CR (2011). A novel elevated plus-maze procedure to avoid the one-trial tolerance problem. *Front Behav Neurosci* **5**, 43.
Sgoifo A, de Boer SF, Westenbroek C, Maes FW, Beldhuis H, Suzuki T & Koolhaas JM (1997). Incidence of arrhythmias and heart rate variability in wild-type rats exposed to social stress. *Am J Physiol* **273**, H1754–H1760.
Shikano Y, Nishimura Y, Okonogi T, Ikegaya Y & Sasaki T (2019). Vagus nerve spiking activity associated with locomotion and cortical arousal states in a freely moving rat. *Eur J Neurosci* **49**, 1298–1312.
Shikano Y, Sasaki T & Ikegaya Y (2018). Simultaneous recordings of cortical local field potentials, electrocardiogram, electromyogram, and breathing rhythm from a freely moving rat. *J Vis Exp* https://doi.org/10.3791/56980.
Tsanov M, Chah E, Reilly R & O'Mara SM (2014). Respiratory cycle entrainment of septal neurons mediates the fast coupling of sniffing rate and hippocampal theta rhythm. *Eur J Neurosci* **39**, 957–974.
Uchida N & Mainen ZF (2003). Speed and accuracy of olfactory discrimination in the rat. *Nat Neurosci* **6**, 1224–1229.
Verhagen JV, Wesson DW, Netoff TI, White JA & Wachowiak M (2007). Sniffing controls an adaptive filter of sensory input to the olfactory bulb. *Nat Neurosci* **10**, 631–639.
Vyazovskiy VV, Olcese U, Lazimy YM, Faraguna U, Esser SK, Williams JC, Cirelli C & Tononi G (2009). Cortical firing and sleep homeostasis. *Neuron* **63**, 865–878.
Wachowiak M (2011). All in a sniff: olfaction as a model for active sensing. *Neuron* **71**, 962–973.
Walf AA & Frye CA (2007). The use of the elevated plus maze as an assay of anxiety-related behavior in rodents. *Nat Protoc* **2**, 322–328.
Watson BO, Levenstein D, Greene JP, Gelinas JN & Buzsaki G (2016). Network homeostasis and state dynamics of neocortical sleep. *Neuron* **90**, 839–852.
Wesson DW (2013). Sniffing behavior communicates social hierarchy. *Curr Biol* **23**, 575–580.
Youngentob SL, Mozell MM, Sheehe PR & Hornung DE (1987). A quantitative analysis of sniffing strategies in rats performing odor detection tasks. *Physiol Behav* **41**, 59–69.

Additional information

Competing interests

The authors declare that they have no competing interests.

Author contributions

All experiments were performed in The University of Tokyo. T.S. designed the study. R.N., Y.S., Y.N. and T.O. acquired the electrophysiological data. N.K. and T.S. performed the analyses, prepared all the figures and wrote the manuscript. Y.I. supervised the project and wrote the manuscript. All the authors reviewed the manuscript. All authors have approved the final version of the manuscript and agree to be accountable for all aspects of the work in ensuring that questions related to the accuracy or integrity of any part of the work are appropriately investigated and resolved. All persons designated as authors qualify for authorship, and all those who qualify for authorship are listed.

Funding

This work was supported by Kaken-hi (19H08497), the Takeda Science Foundation, the Suzuken Memorial Foundation, the Nakatomi Foundation, the Exploratory Research for Advanced Technology (JPMJER1801) and the Precursory Research for Embryonic Science and Technology (JPMJPR1785) from the Japan Science and Technology Agency, and the Advanced Research & Development Programs for Medical Innovation (PRIME) from the Japan Agency for Medical Research and Development.

Keywords

heart rate, local field potential, neocortex, respiration, sniffing